A heterozygous deficiency in protein phosphatase Ppm1b results in an altered ovulation number in mice

NAOKI ISHII[1], TAKUJIRO HOMMA[1], REN WATANABE[2], NAOKO KIMURA[2], MOTOKO OHNISHI[3], TAKAYASU KOBAYASHI[4] and JUNICHI FUJII[1]

[1]Department of Biochemistry and Molecular Biology, Graduate School of Medical Science, Yamagata University, Yamagata, Yamagata 990-9585; [2]Laboratory of Animal Reproduction, Graduate School of Agricultural Sciences, Yamagata University, Tsuruoka, Yamagata 997-8555; [3]Department of Biological Chemistry, College of Bioscience and Biotechnology, Chubu University, Kasugai, Aichi 87-8501; [4]Center for Gene Research, Tohoku University, Sendai, Miyagi 980-8575, Japan

Received October 5, 2018; Accepted April 16, 2019

DOI: 10.3892/mmr.2019.10194

Abstract. Ppm1b, a metal-dependent serine/threonine protein phosphatase, catalyzes the dephosphorylation of a variety of phosphorylated proteins. Ppm1b$^{-/-}$ mouse embryos die at the fertilized oocyte stage, whereas Ppm1b$^{+/-}$ mice with a C57BL/6 background exhibit no phenotypic abnormalities. Because the C57BL/6 strain produces a limited number of pups, in an attempt to produce Ppm1b$^{-/-}$ mice, congenic Ppm1b$^{+/-}$ mice with an ICR background were established, which are more fertile and gave birth to more pups. As a result, however, no Ppm1b$^{-/-}$ offspring were obtained when pairs of Ppm1b$^{+/-}$ ICR mice were bred again. Ppm1b$^{+/-}$ male and female ICR mice were analyzed from the viewpoint of fecundity. The Ppm1b haploinsufficiency had no effect on testicular weight or the number of sperm in male mice. Despite the fact that the levels of Ppm1b protein in the ovaries of sexually mature Ppm1b$^{+/-}$ mice were decreased compared with those of Ppm1b$^{+/+}$ mice, there appeared to be no significant difference in the histological appearance of the ovaries, litter sizes or plasma progesterone levels at the estrous stage. When superovulation was induced by stimulation using a hormone treatment, the number of ovulated oocytes were the same for Ppm1b$^{+/-}$ and Ppm1b$^{+/+}$ mice at 4 weeks of age when the estrous cycle did not proceed, however, the number of ovulated oocytes was lower in sexually mature Ppm1b$^{+/-}$ mice at 11 weeks of age compared with Ppm1b$^{+/+}$ mice in the first and the second superovulation cycles. These collective results suggest that follicle development is excessive in Ppm1b$^{+/-}$ mice, and that this leads to a partial depletion of matured follicles and a corresponding decrease in the number of ovulated oocytes.

Correspondence to: Professor Junichi Fujii, Department of Biochemistry and Molecular Biology, Graduate School of Medical Science, Yamagata University, 2-2-2 Iidanishi, Yamagata, Yamagata 990-9585, Japan
E-mail: jfujii@med.id.yamagata-u.ac.jp

Key words: female fertility, ovary, Ppm1b, protein phosphatase, superovulation

Introduction

Metal-dependent protein phosphatase (PPM), formerly referred to as a member of the protein phosphatase 2C (PP2C) family, is one of two major serine/threonine protein phosphatase families in eukaryotes (1). Ppm1a and Ppm1b, closely related members of the PPM family with an amino acid identity of 75%, catalyze the dephosphorylation of a variety of phosphorylated proteins that are involved in intracellular signaling and cellular responses but show distinct cellular localization (2-4).

Ppm1a catalyzes the dephosphorylation of the p38 mitogen-activated protein kinase (MAPK), MAPK kinase (MKK) 4, MKK6 in the stress-activated protein kinase (SAPK) cascade and Smad2/3 in the bone morhogenic protein (BMP) signaling pathway (5-7), whereas Ppm1b dephosphorylates transforming growth factor (TGF)-β-activated kinase 1 (TAK1), a member of the stress-activated protein kinase (SAPK) cascade (8,9). Ppm1a and Ppm1b also dephosphorylate IκB kinase, a protein kinase that is involved in the nuclear factor kappa κB (NFκB) pathway in cellular systems, and appears to down-regulate or terminate cytokine-induced NFκB activation (10,11). A proteomic analysis has also shown that TNFα enhances the interaction of 14-3-3ε with TAK1 and Ppm1b, suggesting that it is involved in cross talk with the MAPK signaling pathway (12). It therefore appears that Ppm1a and Ppm1b have both unique and redundant functions.

AMP-activated protein kinase (AMPK) is activated in response to increased AMP concentrations and induces the activation of metabolic pathways that generate ATP, while also repressing ATP consumption, and hence can be regarded as a sensor for cellular energy status (13,14). Chida *et al* (15) reported that Ppm1a and Ppm1b dephosphorylate the alpha-subunit of AMPK in their N-myristoylated forms. In addition, Ppm1b activates the peroxisome-proliferator-activated receptor gamma (PPARγ) via the dephosphorylation of Ser^{112} (16). Because PPARγ is a ligand-activated transcriptional factor of

the nuclear receptor superfamily that regulates genes that are involved in differentiation, metabolism, and immunity (17), it is possible that Ppm1b might also be involved in the regulation of these metabolic processes. The association of Ppm1b with glioma amplified sequence 41 (GAS41), a member of a protein family that is characterized by the presence of an N-terminal YEATS domain, catalyzes the dephosphorylation of Ser^{366} of p53, leading to a decrease in p53 levels (18). Because the hyperactivation of p53 causes accelerated senescence, the depletion of Ppm1b causes premature senescence, caused by the sustained activation of p53 (19). Among the five distinct Ppm1b isoforms that are produced by the mouse (20-23), three are predominantly expressed in pachytene spermatocytes and in more highly differentiated germ cells, suggesting that they play a role in the spermatogenic process. The levels of Ppm1b are increased during the course of the first wave of spermatogenesis in the neonatal male mouse (24).

Ppm1b-deficient mice with the C57BL/6 background have been established by a gene-knockout technique (4). Fertilized $Ppm1b^{-/-}$ oocytes die without cleavage, but $Ppm1b^{+/-}$ mice develop normally and show no vast phenotypic abnormalities in the first observation. Since these observations, a Ppm1b gene-trap mouse line ($Ppm1b^{+/d}$), which contains a retroviral gene trap in the second intron of the Ppm1b locus, was developed and employed in studies concerning the Rip3-mediated regulation of necroptosis (25). Homozygous gene-trap mice ($Ppm1b^{d/d}$) are viable and are born with a normal Mendelian distribution. However, these mice express lower levels of the wild-type Ppm1b, which appears to support the viability of the mice.

Because the expression of Ppm1b in germ cells implies that the gene might play a role in reproduction, we attempted to clarify this issue. We changed the genetic background of $Ppm1b^{+/-}$ mice from the C57BL/6 strain to the ICR strain because the latter strain is more fertile and produces more pups. However, no $Ppm1b^{-/-}$ mice were born again, an observation that prompted us to examine the fertilizing ability of $Ppm1b^{+/-}$ mice from the viewpoints of histology and protein levels. The findings indicate that the $Ppm1b^{+/-}$ ICR female mice showed impaired ovulation in response to hormonal stimuli, which is consistent with lower levels of the Ppm1b protein in the ovaries of these mice.

Materials and methods

Animals. Ppm1b-deficient mice were originally generated using embryonic stem cells with a C57BL/6 and b129Sv mixed background using a gene-targeting technique (4). We mated $Ppm1b^{+/-}$ male mice with female congenic ICR mice and backcrossed the litters more than 10 times to produce ICR mice. The animal room climate was maintained under specific pathogen-free conditions at a constant temperature of 20-22˚C with a 12-h alternating light-dark cycle, with food and water available *ad libitum*. The genotype of the mice was determined by polymerase chain reaction (PCR) analysis using specific primers for Ppm1b and knockout allele, as reported previously (4). Animal experiments were performed in accordance with the Declaration of Helsinki under a protocol approved by the Animal Research Committee of Yamagata University.

Assessing reproductive ability of female mice. The fertilizing ability of the $Ppm1b^{+/+}$ and $Ppm1b^{+/-}$ female mice was examined under conventional breeding conditions. Individual $Ppm1b^{+/+}$ and $Ppm1b^{+/-}$ female mouse at 11 weeks old were cohabitated with a sexually mature $Ppm1b^{+/+}$ male mouse and kept until childbirth.

Counting sperm numbers. The number of sperm cells in the cauda epididymis was determined as described in a previous study (26). The cauda epididymis was dissected from the mice, transferred to phosphate buffered saline (PBS), and minced into small pieces. After incubation for 15 min, the released sperm were suspended in the incubation solution to obtain a homogeneous mixture. Sperm numbers were counted under a light microscope.

Immunoblot analyses. The mice were anesthetized by diethyl ether and then sacrificed by thoracotomy and exsanguination. Blood was mostly collected from the heart in the presence of ethylenediaminetetraacetic acid. Animals without reflex but with beating heart were regarded as anaesthetized, and those without heart beat were regarded as dead. Then, testes and ovary were dissected from the dead mice. After dissection, one testis and one ovary from an individual male and female mouse, respectively, were frozen in liquid nitrogen and stored at -80˚C until used. After thawing on ice, the ovaries and testes were homogenized with a glass-teflon homogenizer in lysis buffer, which contained 25 mM Tris-HCl, pH 7.5, 150 mM NaCl, 1% (w/v) Nonidet P-40, 1% (w/v) sodium deoxycholate, and 0.1% (w/v) SDS, supplemented with a protease inhibitor cocktail (P8340, Sigma-Aldrich). After centrifugation at 17,400 x g for 15 min at 4˚C, the protein content in the supernatant was determined using a BCA protein assay reagent (Thermo Fisher Scientific). The proteins (20 μg/lane) were separated on 12 or 15% SDS-polyacrylamide gels and blotted onto polyvinylidene difluoride (PVDF) membranes (GE Healthcare). The blots were blocked with 5% skim milk in Tris-buffered saline containing 0.1% Tween-20 (TBST), and were then incubated overnight with the primary antibodies diluted in TBST containing 1% skim milk. The primary antibodies (diluted 1:1,000) used were; Ppm1b (AF4396, R&D Systems), glyceraldehyde-3-phosphate dehydrogenase (GAPDH) (sc-25778, Santa Cruz Biotechnology), and β-actin (sc-69879, Santa Cruz Biotechnology). After incubation with horseradish peroxidase-conjugated 2nd antibodies (Santa Cruz Biotechnology), the bands were detected using the Immobilon western chemiluminescent HRP substrate (Millipore) on an image analyzer (ImageQuant LAS500, GE Healthcare). After reprobing, the same membranes were reacted with either anti-GAPDH antibody for testicular proteins or anti-β-actin antibody for ovarian proteins because reactivity of the antibodies to non-specific proteins in testes and ovaries was different.

Counting follicles in the whole ovaries. The numbers of follicles in whole ovaries were counted according to a previously described method (27). One ovary from an individual female mouse was used for the analyses. Ovaries were collected from females at 11-weeks of age, fixed in 15% buffered formalin, embedded in paraffin, and 7 μm thick sections were prepared.

Table I. Comparison of female fertility between Ppm1b$^{+/+}$ and Ppm1b$^{+/-}$ ICR mice.

Ppm1b genotype Male x female	Number of mating pairs	Litter size	Number of neonates	
			+/+	+/-
+/+ x +/+	6	14.17±2.32	14.17±2.32	0
+/+ x +/-	14	14.21±2.75	7.50±2.03	6.71±1.94
+/- x +/-	7	13.57±2.57	3.71±1.25	10.00±2.08

Litter sizes and genotype of neonate from indicated genetic pairs of mice were shown. Data are presented as the mean ± standard deviation of indicated number of pairs.

To determine follicle numbers, every 4th serial section was stained with hematoxylin and eosin (H&E). Photographs of the sections were obtained using a BZ-X700 microscope (Keyence) and the number of follicles was counted.

Measurement of plasma progesterone by an enzyme immunoassay. Blood was collected from the tail vein of the mice at the estrous stage in the presence of an excess of ethylenediaminetetraacetic acid. After centrifugation at 800 x g for 5 min, plasma progesterone concentrations in the mice were measured using a Progesterone enzyme-linked immunosorbent assay (ELISA) kit (ADI-900-011, Enzo Life Sciences) according to the manufacturer's instructions.

Oocyte collection after superovulation. Hormone-stimulated ovulation was induced in mice, as described previously (28). Briefly, 4- or 11-week-old Ppm1b$^{+/+}$ and Ppm1b$^{+/-}$ female ICR mice were injected intraperitoneally (i.p.) with 5 IU of pregnant mare serum gonadotropin (PMSG) (Asuka-seiyaku). At 48 h after the administration of PMSG, 5 IU of human chorionic gonadotropin (hCG) (Asuka-seiyaku) was administered i.p. At 14 h after hCG administration, oocytes in the ampullary sites of both fallopian tubes were collected and counted. For repeated-superovulation, PMSG/hCG injections were repeated at interval of 7 days.

Statistical analyses. The results are expressed as the mean ± standard error of the mean (SEM). Statistical analysis was performed using the Student t-test. Data were analyzed by two-way analysis of variance followed by Tukey's multiple comparisons test when comparisons were made in datasets containing more than two groups. All data were analyzed using the GraphPad Prism 6 software. P-values <0.05 were considered to indicate statistically significant differences.

Results

Establishing Ppm1b$^{+/-}$ ICR mice. Ppm1b-deficient mice were originally established under a C57BL/6 background (4), which is commonly used but produces limited numbers of pups compared to the ICR background. We therefore changed the genetic background of the mice from C57BL/6 to ICR mice by mating the original Ppm1b$^{+/-}$ C57BL/6 mice and backcrossing the litters to the ICR mice more than 10 times. However, the breeding of Ppm1b$^{+/-}$ male and Ppm1b$^{+/-}$ female ICR mice under conventional conditions resulted in the birth of only Ppm1b$^{+/+}$ and Ppm1b$^{+/-}$ ICR mice (Table I), an observation that is consistent with the selective death of the Ppmlb$^{-/-}$ embryos reported for mice with the C57BL/6 background (4). Accordingly we analyzed only Ppm1b$^{+/-}$ ICR mice in comparison with Ppm1b$^{+/+}$ ICR mice throughout the study.

Characteristics of Ppm1b$^{+/-}$ male ICR mice. We first examined sexually mature male mice because the involvement of Ppm1b in the spermatogenic process was suspected, based on the unique expression of isoforms in spermatogenic cells (20-23). Generally male mice are sexually matured after 8 weeks, so that we chose mice at 11 weeks old when they were fully matured and most reproductive. Ppm1b$^{+/-}$ male ICR mice were viable, with normal growth and showed no obvious abnormalities. The body weights of the Ppm1b$^{+/-}$ male ICR mice and Ppm1b$^{+/+}$ male ICR mice at 11-weeks of age were identical (Fig. 1A). No significant difference in testes weight (Fig. 1B) or sperm numbers (Fig. 1C) was detected between Ppm1b$^{+/-}$ and Ppm1b$^{+/+}$ male ICR mice, which is consistent with results reported for mice with the C57BL/6 background (4). The antibody against Ppm1b indicated the presence of two bands corresponding to 43 and 53 kDa in size in all testes, irrespective of the mouse genotype. The 53-kDa protein is the form that is expressed ubiquitously, and the 43-kDa protein is the form that is expressed specifically in the testis and liver (20-23). While the expression of two out of five Ppm1 isoforms could be confirmed, the levels of both the 43 and 53-kDa Ppm1b proteins in the testes were not significantly different between Ppm1b$^{+/+}$ and Ppm1b$^{+/-}$ mice at 11-weeks of age (Fig. 1D). It therefore appears that the Ppm1b$^{+/-}$ male ICR mice are normal in terms of spermatogenesis.

Ovarian expression of Ppm1b in mice. Ppm1b$^{+/-}$ female ICR mice also developed normally and had normal body and ovary weights compared with the age-matched Ppm1b$^{+/+}$ female ICR mice (Fig. 2). We then performed immunoblot analyses of proteins isolated from the ovaries. An antibody against Ppm1b indicated the presence of a band corresponding to a size of 53 kDa from all ovaries. The levels of the Ppm1b protein in ovaries were not significantly different between Ppm1b$^{+/+}$ and Ppm1b$^{+/-}$ mice at 4-weeks of age (Fig. 3A). However, it was down-regulated to about 50% in the Ppm1b$^{+/-}$ mice compared to the Ppm1b$^{+/+}$ mice at 11-weeks of age (Fig. 3B). Thus, the expression of the Ppm1b gene appeared to be altered during

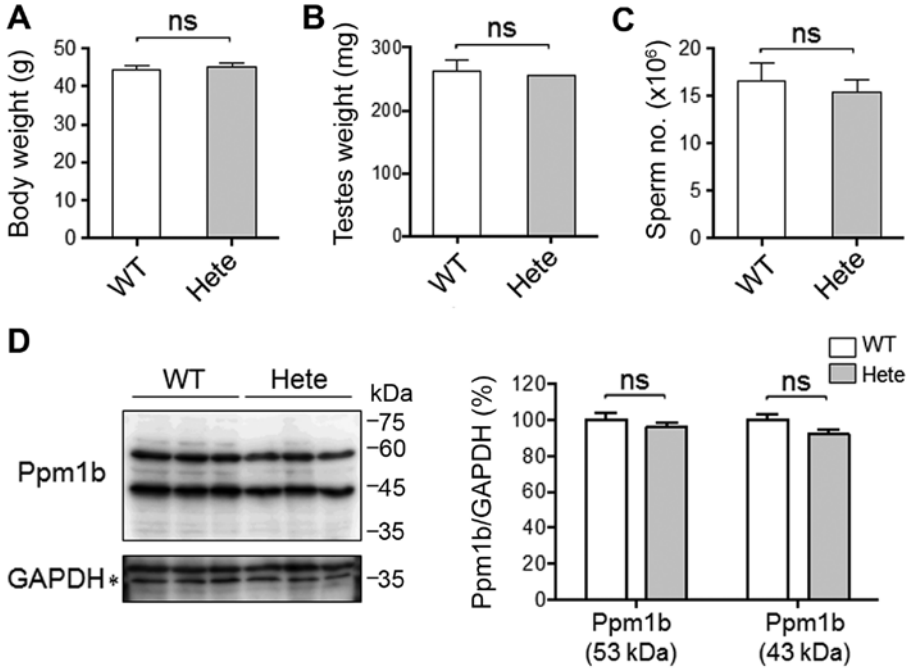

Figure 1. Characteristics of Hete male ICR mice. (A) Body weight, (B) testes weight, and (C) epididymal sperm numbers of WT and Hete ICR mice at 11-weeks of age. Data are presented as the mean ± SEM (n=4 per genotype). (D) Proteins were isolated from the testes of the WT and Hete ICR mice at 11 weeks old and were subjected to immunoblot analyses using antibodies against Ppm1b and GAPDH. The asterisk represents a nonspecific band. Left panels, representative blots are shown. Right graph, immune reactive bands were semi-quantified by scanning the blot membranes and normalized to GAPDH. Data are presented as the mean ± SEM (n=3). ns, not significant; WT, Ppm1b$^{+/+}$; Hete, Ppm1b$^{+/-}$; GAPDH, glyceraldehyde-3-phosphate dehydrogenase.

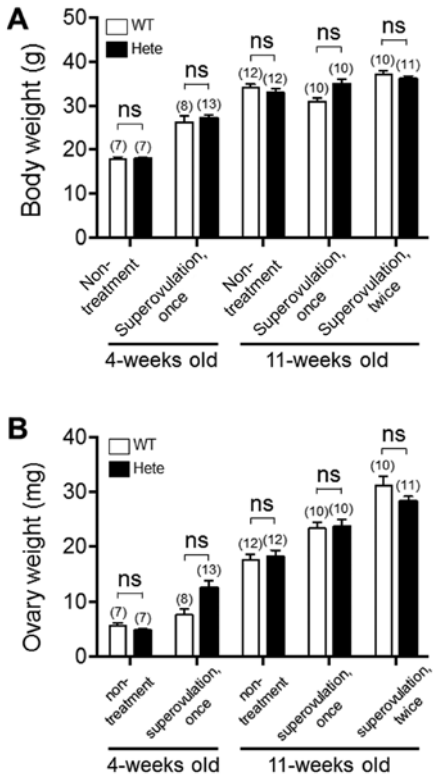

Figure 2. Changes in body and ovary weights following superovulation. WT and Hete female ICR mice at the indicated ages were superovulated once (4- and 11-week old mice) or twice (11-week old mice). (A) Body weight and (B) ovary weight of WT and Hete ICR mice were shown. The number of female mice used for each treatment is shown within parentheses above the columns. The data on the superovulated mice came from the same mice presented as Fig. 4. Data were analyzed by two-way analysis of variance followed by Tukey's multiple comparisons test. Data were presented as the mean ± SEM. ns, not significant; WT, Ppm1b$^{+/+}$; Hete, Ppm1b$^{+/-}$.

the sexual maturation of the ovaries, suggesting the existence of a haploinsufficiency of the gene at the sexually mature stage.

Characteristics of Ppm1b$^{+/-}$ female ICR mice. Because Ppm1b was down-regulated in Ppm1b$^{+/-}$ ovaries at 11-weeks of age, we hypothesized that ovary structure and/or function may have been altered. We performed a histological analysis of ovaries from mice at 11-weeks of age. H&E-stained ovarian sections from the Ppm1b$^{+/-}$ ICR mice appeared to be similar to those from the Ppm1b$^{+/+}$ ICR mice (data not shown). The same numbers of offspring were produced when Ppm1b$^{+/+}$ and Ppm1b$^{+/-}$ female ICR mice were mated with Ppm1b$^{+/+}$ male ICR mice (Fig. 3C), which suggests that Ppm1b$^{+/-}$ female ICR mice have a normal fertility. In addition, no differences in plasma progesterone levels were detected at the estrous stage of the mice (Fig. 3D).

The number of ovulated oocytes by superovulation is reduced in Ppm1b$^{+/-}$ ICR mice. Because the process of ovulation is similar to inflammation that accompanies oxidative stress with elevated reactive oxygen and nitrogen species (29), the induction of ovulation may expose a latent impairment caused by a Ppm1b haploinsufficiency. To address this issue, we evaluated ovarian function under conditions of superovulation by administering PMSG followed by hCG to stimulate ovulation (a well-accepted protocol) (28) in female mice at 4- and 11-weeks of age. After superovulation, the weights of ovaries from the Ppm1b$^{+/-}$ ICR mice were found to be similar to those from the Ppm1b$^{+/+}$ ICR mice (Fig. 2B) and no difference was found in the number of ovulated oocytes at 4-weeks of age (Fig. 4A). However, at 11-weeks of age the number of ovulated oocytes was smaller in the Ppm1b$^{+/-}$ ICR mice compared to

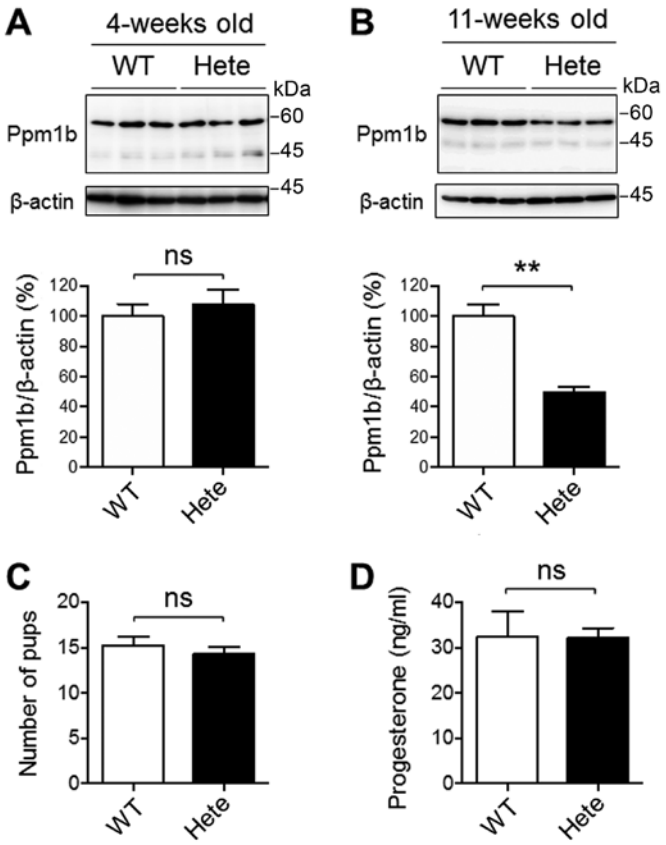

Figure 3. Characteristics of Hete female ICR mice. Proteins were isolated from the ovaries of the WT and Hete ICR mice at the ages of (A) 4-weeks or (B) 11-weeks and were subjected to immunoblot analyses using antibodies against Ppm1b and β-actin. Upper panels, representative blots were shown. Lower graphs, immune reactive bands were semi-quantified by scanning the blot membranes and normalized to β-actin. Data were presented as the mean ± SEM, n=3. (C) Litter size of WT and Hete female ICR mice (11- to 13-week-old) mated with a WT male ICR mouse. Data were presented as the mean ± SEM (WT, n=8; Hete, n=7). (D) Plasma progesterone levels in 11-week-old WT and Hete female ICR mice at the estrous stage. Data were presented as the mean ± SEM (n=4). **P<0.01. ns, not significant; WT, Ppm1b$^{+/+}$; Hete, Ppm1b$^{+/-}$.

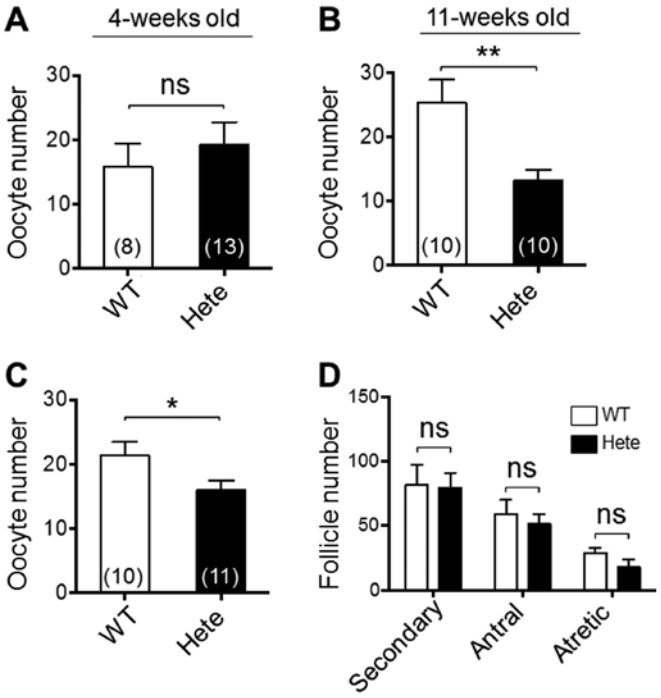

Figure 4. Number of oocytes produced by superovulation and developed follicles in the ovaries of WT and Hete female ICR mice. The number of ovulated oocytes from WT and Hete female ICR mice at the ages of (A) 4-weeks or (B) 11-weeks subjected to one cycle of hormone treatment. (C) The number of ovulated oocytes from WT and Hete female ICR mice (11-weeks old) subjected to two cycles of hormone treatment. The numbers of oocytes collected were expressed as the mean ± SEM. The number of female mice used for each treatment is shown in parentheses within the columns. (D) The number of follicles in ovaries were counted on sections of whole ovaries of the mice (11-weeks old). Data were presented as the mean ± SEM (n=4). *P<0.05, **P<0.01. The data were analyzed using the Students t-test. ns, not significant; WT, Ppm1b$^{+/+}$; Hete, Ppm1b$^{+/-}$.

the Ppm1b$^{+/+}$ ICR mice (Fig. 4B), although no difference was observed in ovary weight (Fig. 2B). Interestingly, the number of ovulated oocytes caused by the hormone treatment remained less in Ppmlb$^{+/-}$ ICR mice at the second superovulation (Fig. 4C). Although the macroscopic appearance of the ovaries was normal (data not shown), the decreased ovulation could have been caused by impaired folliculogenesis in the Ppm1b$^{+/-}$ ICR mice. We attempted to validate this possibility by counting follicles in whole ovaries at the developed stages. The results indicated that the number of follicles at stages later than the secondary follicle in whole ovaries were similar between these genotypic mice (Fig. 4D). Thus, the hormone treatment stimulated the ovulation process, but not folliculogenesis, an observation that appears to be due to a defect resulting from a haploinsufficiency of the Ppm1b gene.

Discussion

We found that the number of ovulated oocytes resulting from stimulation by a hormone treatment were lower in sexually mature Ppm1b$^{+/-}$ female ICR mice at 11-weeks of age compared to Ppm1b$^{+/+}$ ICR mice but were essentially the same in immature mice at 4-weeks of age (Fig. 4). It therefore appears that a haploinsufficiency of the Ppm1b gene exerted an influence over the Ppm1b protein only in ovaries from sexually mature female mice at 11-weeks of age (Fig. 3). Thus, Ppm1b expression may be regulated, at least in part, by female sex hormones. However, there were no differences in the histological appearance of the ovaries, litter sizes, or plasma progesterone levels at the estrous stage, even in mice at 11-weeks of age (Fig. 3). Although we did not perform precise examination on ovarian function due to limited amounts of samples, evaluation of basic ovarian function by measuring hallmarks, such as anti-Müllerian hormone (AMH), might help understanding roles of Ppm1b. There appears to be a correlation between the number of ovulated oocytes by superovulation and protein levels of Ppm1b in ovaries, although the precise mechanism responsible for the Ppm1b gene expression is not clear at this stage of our studies. Thus, the results obtained herein suggest that Ppm1b plays roles in the ovulation process in response to hormones.

Contrary to the impaired reproductive ability of female mice, there were no differences in sperm numbers and other phenotypes between Ppm1b$^{+/+}$ and Ppm1b$^{+/-}$ male ICR mice (Fig. 1). We detected two Ppm1 protein bands that were different in size and which corresponded to the Ppm1b isoforms that are specifically expressed in differentiated male

germ cells (20-23). The levels of the Ppm1b isoforms were the same between $Ppm1b^{+/+}$ and $Ppm1b^{+/-}$ male ICR mice, suggesting that a haploinsufficiency of the Ppm1b gene neither affected the expression of these two isoforms nor the phenotypes in the male reproductive system. The pool of primordial follicles is maintained in a dormant state by a variety of inhibitory machinery for follicular activation, including phosphatase and a tensin homolog deleted on chromosome ten (PTEN) and Foxo3a, and the loss of function of the inhibitory molecule leads to the premature activation of the primordial follicle pool and follicle depletion (30). The excessive activation of the mammalian target of rapamycin complex 1 (mTORC1) actually causes an accelerated activation and the depletion of primordial follicles in mouse ovaries (31,32). It has been reported that the pharmacological inhibition of mTORC1 activity by a rapamycin treatment consistently leads to the suppression of primordial follicle activation (33). Based on these findings, we hypothesized that a haploinsufficiency of the Ppm1b gene might have caused the decline in the number of follicles and decreased numbers of ovulated oocytes in the $Ppm1b^{+/-}$ ICR mice. However, no difference was found in the number of developed follicles between ovaries from $Ppm1b^{+/-}$ and $Ppm1b^{+/+}$ mice (Fig. 4D). Thus, these collective results suggest an opposite scenario; i.e. follicle development proceeds at an excessive level in the $Ppm1b^{+/-}$ mice, leading to the partial depletion of matured follicles and a decrease in the number of ovulated oocytes. This issue will need to be clarified in a future study.

Hormonal stimuli with PMSG and hCG induces the activation of a variety of processes, including steroidogenesis, and releases progesterone to maintain pregnancy (34). Steroidogenesis involves several enzymatic processes, including oxygenase reactions that are mediated by the P450 side-chain cleavage enzyme (P450scc) (35). Reactive oxygen species (ROS) are produced as byproducts of these oxygenase-catalyzed reactions and the action of molecules that are susceptible to oxidation are impaired (36), as is typically seen in the redox reactive molecule peroxiredoxin (37). In addition, hydrogen peroxide, a stable and less toxic ROS, can regulate hormonal responses via its ability to modulate redox-sensitive machinery such as epidermal growth factor (EGF)-receptor signaling (38). Because tyrosine phosphatases contain a redox-sensitive sulfhydryl residue at the catalytic center and is prone to oxidative inactivation, hydrogen peroxide that is produced by NADPH oxidases stimulate the signaling pathway, as demonstrated in the case of EGF receptor signaling (39). However, Ppm1b is a metal-dependent protein phosphatase that catalyzes the dephosphorylation of phospho-serine/threonine in proteins (1) and is less sensitive to oxidative modification than phosphotyrosine phosphatases. This suggests that the direct inactivation of Ppm1b by ROS would be less likely.

Because many protein kinases catalyze the phosphorylation of hydroxyl groups of serine/threonine residues in signaling proteins, as typified in the MAPK cascade (3,5-7), a dysfunction in Ppm1b may sustain the phosphorylation process active state and enhance cellular proliferation after hormonal stimuli. The interaction between mTOR and the MAPK signaling pathways and their participation in the ovulation process is complex and is currently not fully understood (40). The findings reported herein suggest that the process is regulated by the dephosphorylation via Ppm1b and is functional during ovulation in response to hormonal stimulation. Experiments using conditional Ppm1b-null knockout mice would provide a clear picture of this issue as well as the *bona fide* roles of Ppm1b. In fact, for unknown reasons, we, as well as Sasaki *et al* (4) have made numerous attempts to establish conditional knockout mice but failed to obtain $Ppm1b^{flox/flox}$ mice, which are required if Ppm1b gene is to be deleted conditionally. Because a haploinsufficiency of Ppm1b resulted in a decreased number of ovulated oocytes by superovulation (Fig. 4), agents that activate Ppm1b may be a beneficial agent for increasing the number of ovulated oocytes and consequently litter sizes. Ppm1b reportedly dephosphorylates Pax2, which encodes the protein required for the development of several organs in embryos, and results in switching Pax2 from a transcriptional activator to a repressor protein (41). The ablation of Ppm1b sustains the phosphorylation of the tumor suppressor gene, the retinoblastoma gene (RB1), and down regulates U2OS osteosarcoma cell growth (42). Thus, Ppm1b appears to support the proliferation of tumor cells. On the contrary, the knockdown of Ppm1b activates Rho GTPase, which results in the invasion and migration of breast cancer cells (43), suggesting that Ppm1b has a suppressive function in these cells. Thus, the functional consequence of Ppm1b largely depends on the types of cells, and a complete understanding of its roles are awaited for the purpose of improved female reproduction and cancer therapy.

In conclusion, we report herein that a heterozygous deficiency of the Ppm1b gene in female ICR mice results in a deteriorated response in hormone-stimulated ovulation. The identification of the target proteins of Ppm1b should provide clues to our understanding of the phosphorylation-dephosphorylation reactions that regulate the ovulation process in the ovary in response to hormonal stimuli.

Acknowledgements

The authors would like to thank Mr. Tsunekata Ito (Animal Center, Institute for Promotion of Medical Science Research, Faculty of Medicine, Yamagata University, Yamagata, Japan) for providing advice on animal handling.

Funding

This work was partly supported by the Cooperative Research Project Program of the Joint Usage/Research Center at the Institute of Development, Aging and Cancer, Tohoku University (grant no. 2012-4).

Availability of data and materials

The datasets used and/or analyzed during the current study are available from the corresponding author on reasonable request.

Authors' contributions

NI performed the majority of the experiments. TH, RW and NK assisted with some experiments. MO and TK established the $Ppm1b^{+/-}$ mice and provided them for this study. JF

designed the study, interpreted data, drafted the manuscript and revised it critically for important intellectual content. All authors read and approved the final manuscript.

Ethics approval and consent to participate

The study included animal experiments only. Animal experiments were performed in accordance with the Declaration of Helsinki under a protocol approved by the Animal Research Committee of Yamagata University.

Patient consent for publication

Not applicable.

Competing interests

The authors declare that they have no competing interests.

References

1. Shi Y: Serine/threonine phosphatases: Mechanism through Structure. Cell 139: 468-484, 2009.
2. Lifschitz-Mercer B, Sheinin Y, Ben-Meir D, Bramante-Schreiber L, Leider-Trejo L, Karby S, Smorodinsky NI and Lavi S: Protein phosphatase 2Calpha expression in normal human tissues: An immunohistochemical study. Histochem Cell Biol 116: 31-39, 2001.
3. Lin X, Duan X, Liang YY, Su Y, Wrighton KH, Long J, Hu M, Davis CM, Wang J, Brunicardi FC, *et al*: PPM1A functions as a Smad phosphatase to terminate TGF-beta signaling. Cell 125: 915-928, 2006.
4. Sasaki M, Ohnishi M, Tashiro F, Niwa H, Suzuki A, Miyazaki J, Kobayashi T and Tamura S: Disruption of the mouse protein Ser/Thr phosphatase 2Cbeta gene leads to early pre-implantation lethality. Mech Dev 124: 489-499, 2007.
5. Takekawa M, Maeda T and Saito H: Protein phosphatase 2Calpha inhibits the human stress-responsive p38 and JNK MAPK pathways. EMBO J 17: 4744-4752, 1998.
6. Duan X, Liang YY, Feng XH and Lin X: Protein serine/threonine phosphatase PPM1A dephosphorylates Smad1 in the bone morphogenetic protein signaling pathway. J Biol Chem 281: 36526-36532, 2006.
7. Dai F, Shen T, Li Z, Lin X and Feng XH: PPM1A dephosphorylates RanBP3 to enable efficient nuclear export of Smad2 and Smad3. EMBO Rep 12: 1175-1181, 2011.
8. Hanada M, Kobayashi T, Ohnishi M, Ikeda S, Wang H, Katsura K, Yanagawa Y, Hiraga A, Kanamaru R and Tamura S: Selective suppression of stress-activated protein kinase pathway by protein phosphatase 2C in mammalian cells. FEBS Lett 437: 172-176, 1998.
9. Hanada M, Ninomiya-Tsuji J, Komaki K, Ohnishi M, Katsura K, Kanamaru R, Matsumoto K and Tamura S: Regulation of the TAK1 signaling pathway by protein phosphatase 2C. J Biol Chem 276: 5753-5759, 2001.
10. Prajapati S, Verma U, Yamamoto Y, Kwak YT and Gaynor RB: Protein phosphatase 2Cbeta association with the IkappaB kinase complex is involved in regulating NF-kappaB activity. J Biol Chem 279: 1739-1746, 2004.
11. Sun W, Yu Y, Dotti G, Shen T, Tan X, Savoldo B, Pass AK, Chu M, Zhang D, Lu X, *et al*: PPM1A and PPM1B act as IKKbeta phosphatases to terminate TNFalpha-induced IKKbeta-NF-kappaB activation. Cell Signal 21: 95-102, 2009.
12. Zuo S, Xue Y, Tang S, Yao J, Du R, Yang P and Chen X: 14-3-3 epsilon dynamically interacts with key components of mitogen-activated protein kinase signal module for selective modulation of the TNF-alpha-induced time course-dependent NF-kappaB activity. J Proteome Res 9: 3465-3478, 2010.
13. Hardie DG: AMP-activated protein kinase: An energy sensor that regulates all aspects of cell function. Genes Dev 25: 1895-1908, 2011.
14. Carling D, Mayer FV, Sanders MJ and Gamblin SJ: AMP-activated protein kinase: Nature's energy sensor. Nat Chem Biol 7: 512-518, 2011.
15. Chida T, Ando M, Matsuki T, Masu Y, Nagaura Y, Takano-Yamamoto T, Tamura S and Kobayashi T: N-Myristoylation is essential for protein phosphatases PPM1A and PPM1B to dephosphorylate their physiological substrates in cells. Biochem J 449: 741-749, 2013.
16. Tasdelen I, van Beekum O, Gorbenko O, Fleskens V, van den Broek NJF, Koppen A, Hamers N, Berger R, Coffer PJ, Brenkman AB and Kalkhoven E: The serine/threonine phosphatase PPM1B (PP2Cβ) selectively modulates PPARγ activity. Biochem J 451: 45-53, 2013.
17. Tontonoz P and Spiegelman BM: Fat and beyond: The diverse biology of PPARgamma. Annu Rev Biochem 77: 289-312, 2008.
18. Park JH, Smith RJ, Shieh SY and Roeder RG: The GAS41-PP2Cbeta complex dephosphorylates p53 at serine 366 and regulates its stability. J Biol Chem 286: 10911-10917, 2011.
19. Park JH, Hale TK, Smith RJ and Yang T: PPM1B depletion induces premature senescence in human IMR-90 fibroblasts. Mech Ageing Dev 138: 45-52, 2014.
20. Wenk J, Trompeter HI, Pettrich KG, Cohen PT, Campbell DG and Mieskes G: Molecular cloning and primary structure of a protein phosphatase 2C isoform. FEBS Lett 297: 135-138, 1992.
21. Terasawa T, Kobayashi T, Murakami T, Ohnishi M, Kato S, Tanaka O, Kondo H, Yamamoto H, Takeuchi T and Tamura S: Molecular cloning of a novel isotype of Mg(2+)-dependent protein phosphatase beta (type 2C beta) enriched in brain and heart. Arch Biochem Biophys 307: 342-349, 1993.
22. Hou EW, Kawai Y, Miyasaka H and Li SS: Molecular cloning and expression of cDNAs encoding two isoforms of protein phosphatase 2C beta from mouse testis. Biochem Mol Biol Int 32: 773-780, 1994.
23. Kato S, Terasawa T, Kobayashi T, Ohnishi M, Sasahara Y, Kusuda K, Yanagawa Y, Hiraga A, Matsui Y and Tamura S: Molecular cloning and expression of mouse mg(2+)-dependent protein phosphatase beta-4 (type 2C beta-4). Arch Biochem Biophys 318: 387-393, 1995.
24. Kato S, Kobayashi T, Kusuda K, Nishina Y, Nishimune Y, Yomogida K, Yamamoto M, Sakagami H, Kondo H, Ohnishi M, *et al*: Differentiation-dependent enhanced expression of protein phosphatase 2Cbeta in germ cells of mouse seminiferous tubules. FEBS Lett 396: 293-297, 1996.
25. Chen W, Wu J, Li L, Zhang Z, Ren J, Liang Y, Chen F, Yang C, Zhou Z, Su SS, *et al*: Ppm1b negatively regulates necroptosis through dephosphorylating Rip3. Nat Cell Biol 17: 434-444, 2015.
26. Iuchi Y, Okada F, Tsunoda S, Kibe N, Shirasawa N, Ikawa M, Okabe M, Ikeda Y and Fujii J: Peroxiredoxin 4 knockout results in elevated spermatogenic cell death via oxidative stress. Biochem J 419: 149-158, 2009.
27. Myers M, Britt KL, Wreford NGM, Ebling FJP and Kerr JB: Methods for quantifying follicular numbers within the mouse ovary. Reproduction 127: 569-580, 2004.
28. Kimura N, Tsunoda S, Iuchi Y, Abe H, Totsukawa K and Fujii J: Intrinsic oxidative stress causes either 2-cell arrest or cell death depending on developmental stage of the embryos from SOD1-deficient mice. Mol Hum Reprod 16: 441-451, 2010.
29. Jabbour HN, Sales KJ, Catalano RD and Norman JE: Inflammatory pathways in female reproductive health and disease. Reproduction 138: 903-919, 2009.
30. Adhikari D and Liu K: Molecular mechanisms underlying the activation of mammalian primordial follicles. Endocr Rev 30: 438-464, 2009.
31. Adhikari D, Flohr G, Gorre N, Shen Y, Yang H, Lundin E, Lan Z, Gambello MJ and Liu K: Disruption of Tsc2 in oocytes leads to overactivation of the entire pool of primordial follicles. Mol Hum Reprod 15: 765-770, 2009.
32. Adhikari D, Zheng W, Shen Y, Gorre N, Hämäläinen T, Cooney AJ, Huhtaniemi I, Lan ZJ and Liu K: Tsc/mTORC1 signaling in oocytes governs the quiescence and activation of primordial follicles. Hum Mol Genet 19: 397-410, 2010.
33. Tong Y, Li F, Lu Y, Cao Y, Gao J and Liu J: Rapamycin-sensitive mTORC1 signaling is involved in physiological primordial follicle activation in mouse ovary. Mol Reprod Dev 80: 1018-1034, 2013.
34. Light A and Hammes SR: Membrane receptor cross talk in steroidogenesis: Recent insights and clinical implications. Steroids 78: 633-638, 2013.
35. Mizutani T, Ishikane S, Kawabe S, Umezawa A and Miyamoto K: Transcriptional regulation of genes related to progesterone production. Endocr J 62: 757-763, 2015.

36. Yasui H, Hayashi S and Sakurai H: Possible involvement of singlet oxygen species as multiple oxidants in p450 catalytic reactions. Drug Metab Pharmacokinet 20: 1-13, 2005.
37. Rhee SG, Woo HA, Kil IS and Bae SH: Peroxiredoxin functions as a peroxidase and a regulator and sensor of local peroxides. J Biol Chem 287: 4403-4410, 2012.
38. Finkel T: Signal transduction by reactive oxygen species. J Cell Biol 194: 7-15, 2011.
39. Bae YS, Oh H, Rhee SG and Yoo YD: Regulation of reactive oxygen species generation in cell signaling. Mol Cells 32: 491-509, 2011.
40. Siddappa D, Kalaiselvanraja A, Bordignon V, Dupuis L, Gasperin BG, Roux PP and Duggavathi R: Mechanistic target of rapamycin (MTOR) signaling during ovulation in mice. Mol Reprod Dev 81: 655-665, 2014.
41. Abraham S, Paknikar R, Bhumbra S, Luan D, Garg R, Dressler GR and Patel SR: The Groucho-associated phosphatase PPM1B displaces Pax transactivation domain interacting protein (PTIP) to switch the transcription factor Pax2 from a transcriptional activator to a repressor. J Biol Chem 290: 7185-7194, 2015.
42. Miller RE, Uwamahoro N and Park JH: PPM1B depletion in U2OS cells supresses cell growth through RB1-E2F1 pathway and stimulates bleomycin-induced cell death. Biochem Biophys Res Commun 500: 391-397, 2018.
43. Cho HJ, Kim JT, Lee SJ, Hwang YS, Park SY, Kim BY, Yoo J, Hong KS, Min JK, Lee CH, *et al*: Protein phosphatase 1B dephosphorylates Rho guanine nucleotide dissociation inhibitor 1 and suppresses cancer cell migration and invasion. Cancer Lett 417: 141-151, 2018.